

A Phase Field Description of Spatio-Temporal Behavior in Thin Liquid Layers

Rodica Borgia¹ and Michael Bestehorn²

Abstract: We study numerically the fully nonlinear evolution of thin liquid films on solid supports in three spatial dimensions. A phase field model is used as mathematical tool. Homogeneous and inhomogeneous substrates are taken into account. For flat homogeneous substrates the stability of thin liquid layers is investigated under the action of gravity. The coarsening process at the solid boundary can be controlled on inhomogeneous substrates. On substrates chemically patterned in an adequate way with hydrophobic and hydrophilic spots (functional surfaces), one can obtain stable regular liquid droplets as final dewetted morphology.

Keywords: Dewetting phenomena, Drop formation, Controlled pattern formation, Interface and Surface Thermodynamics

1 Introduction

Spatio-temporal behavior of thin liquid layers on a solid support has widespread technological applications like coating/wetting phenomena (Gennes 1985; Starov *et al.* 2007, and references therein) and opens new strategies for designing smart microfluidic devices (Alexeev and Balazs 2007).

If the free surface of the flat film is unstable to spatial disturbances, pattern formation sets in and drops, holes and eventually film rupture may occur. In a thin liquid layer one finds after a while the formation of larger and larger structures, a phenomenon known as coarsening. The dynamics converges to a stationary state which consists in a single elevation (drop) or suppression (hole) of the surface. This development can be interrupted by rupture of the film. Rupture is obtained if the surface touches the substrate and the thickness reaches zero in a certain domain. One can avoid rupture by introducing a repelling disjoining pressure (caused

¹ Email: borcia@physik.tu-cottbus.de, Lehrstuhl Statistische Physik / Nichtlineare Dynamik, Brandenburgische Technische Universität Cottbus, Erich-Weinert-Straße 1, 03046, Cottbus, Germany

² Lehrstuhl Statistische Physik / Nichtlineare Dynamik, Brandenburgische Technische Universität Cottbus, Erich-Weinert-Straße 1, 03046, Cottbus, Germany

by van der Waals forces) acting in very thin liquid layers with heights in the range of $1 - 100 \text{ nm}$. In this situation a completely dry region cannot exist. The substrate is covered by a so-called precursor film. The precursor film is stabilized by the disjoining pressure in the evolution equation for the film thickness and is controlled by the Hamaker constant. Including the repelling disjoining pressure at the solid substrate, pattern formation in two and three dimensions was intensively studied in the long-time limit using the long-wave-approach (see, e.g., Bestehorn and Neuffer 2001; Scheid *et al.* 2002; Bestehorn *et al.* 2003; Pototsky *et al.* 2004; Pismen and Thiele 2006). Using a lubrication approximation, this approach is valid only for small velocities and small contact angles (hydrophilic surfaces).

Our aim is to study the behavior of thin liquid films on both hydrophilic and hydrophobic surfaces using a phase field model. The phase field models introduce an order parameter that thermodynamically describes the phases. For a liquid-vapor system we chose the density ρ as order parameter. $\rho = 1$ denotes the liquid phase, and $\rho = 0$ denotes the vapor phase. The wettability properties at the substrate as well as the static contact angle θ and the thickness of the precursor film are controlled by the density at the solid boundary ρ_S , a free parameter between 0 and 1 (see Pismen and Pomeau 2000; Borcia *et al.* 2008)

$$\cos \theta = -1 + 6 \rho_S^2 - 4 \rho_S^3.$$

$\rho_S = 0$ means that there is no-precursor film at the substrate (no-wetting case), and $\rho_S = 1$ corresponds to the largest precursor film (complete wetting). Large values for ρ_S ($\rho_S > 0.5$) correspond to small contact angles ($\theta < 90^\circ$) and vice-versa. No restrictions regarding small or large contact angles appear within the phase field formalism.

The outline of the paper is as follows: The phase field formulation for a liquid-vapor system is briefly depicted in Sec. 2. The stability of a thin liquid film on a flat homogeneous solid substrate with variable wettability under gravity effects is discussed in Sec. 3. Computer simulations in three spatial dimensions for dewetting phenomena/drop formation and controlled pattern formation on functional surfaces are presented in Sec. 4. We gather the conclusions in Sec. 5.

2 Phase field equations

In the phase field model the interface is introduced implicitly by gradients of the phase field in the free-energy functional of the system (see, e.g., Pismen and Pomeau 2000; Bray 1994; Jasnow and Viñals 1996)

$$\mathcal{F}[\rho] = \int_V \left[f(\rho) + \frac{\mathcal{K}}{2} (\nabla \rho)^2 \right] dV, \quad (1)$$

where the first term represents the free-energy density for the homogeneous phases. For a system in equilibrium and without interfacial mass exchange the free-energy density has the form of a double-well potential with two minima corresponding to the two alternative phases: $\rho = 1$ (liquid) and $\rho = 0$ (vapor bulk). We take

$$f(\rho) = \frac{C}{2}\rho^2(\rho - 1)^2 \quad (2)$$

with C being a characteristic value of the free-energy density $f(\rho)$. The second term in (1) is a "gradient energy" which is a function of the local state.

The specific interfacial free-energy γ is, by definition, the difference per unit area of interface between the actual free energy of the system and that which it would have if the properties of the phases were continuous throughout. Hence the free-energy excess of the interface takes the form (Cahn and Hilliard 1958)

$$\gamma = \int_{-\infty}^{+\infty} \mathcal{K} \left(\frac{\partial \rho}{\partial z} \right)^2 dz, \quad (3)$$

which gives a direct connection between the surface tension coefficient γ and the gradient energy term $\mathcal{K}(\partial\rho/\partial z)^2/2$ (where \mathcal{K} is the square gradient parameter).

The basic equations consist of the Navier-Stokes equations including phase field gradient terms for assuring the shear stress balance at the interface

$$\begin{aligned} \rho \frac{d\vec{v}}{dt} = & -\nabla p + \rho \nabla (\nabla \cdot (\mathcal{K} \nabla \rho)) + \nabla \cdot (\eta \nabla \vec{v}) \\ & + \nabla \left(\frac{\eta}{3} \nabla \cdot \vec{v} \right) + \rho \vec{g} \end{aligned} \quad (4)$$

and the continuity equation

$$\frac{\partial \rho}{\partial t} + \nabla \cdot (\rho \vec{v}) = 0. \quad (5)$$

In (4), $\frac{d\vec{v}}{dt}$ represents the total derivative of the velocity field \vec{v} , $p = \rho \partial f(\rho)/\partial \rho - f(\rho)$ is the thermodynamical pressure, η is the dynamic viscosity, and g the gravitational acceleration. The second term on the right-hand-side denotes the Korteweg stress introduced first in Korteweg (1901) and studied latter in Borcia and Bestehorn (2003); Bessonov *et al.* (2004); Borcia and Bestehorn (2005); Pojman *et al.* (2006), and references therein. This term describes the contribution of capillary forces and substitutes into the phase field model the classical boundary condition for tangential stresses at the liquid-vapor interface (Borcia and Bestehorn 2003).

We scale the variables by using d , d^2/ν_l , ν_l/d as units for the length, time and velocity where $d = \sqrt{\mathcal{K}/C}$ represents the characteristic thickness of the diffuse

interface and ν_l is the liquid kinematic viscosity. The following non-dimensional parameters appear: $C_a = \mathcal{K} / \rho_l \nu_l^2$ – the capillary number and $G = g d^3 / \nu_l^2$ – the gravitation number (ρ_l – the liquid density). The surface tension coefficient can be related to C and \mathcal{K} as $\gamma \approx \sqrt{KC}$ (see Pismen and Pomeau 2000). For the numerical results presented in this paper, we have $C_a = 5$ and $G = 10^{-4}$.

3 Chemical potential. Maxwell construction

The stability of a flat liquid film on a solid support can be understood in terms of the dependence of the chemical potential on the film thickness. Pismen and Pomeau (2000) formulated a continuum model describing the liquid layer behavior in the vicinity of the three-phase contact line (solid-liquid-vapor). Starting from the Euler-Lagrange formalism, they considered an expression for the chemical potential

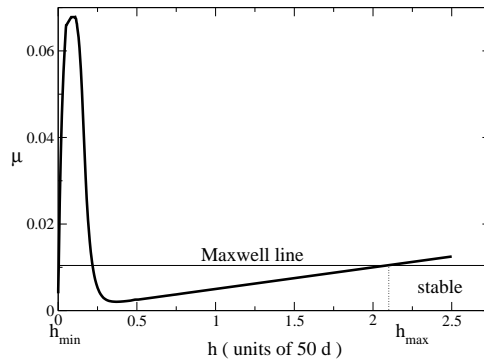
$$\mu = \frac{\partial f}{\partial \rho} - \frac{\partial^2 \rho}{\partial z^2} + Gz. \quad (6)$$

We solve (6) numerically under the boundary conditions $\rho(z=0) = \rho_s$ and $\rho(z \rightarrow \infty) = 0$.

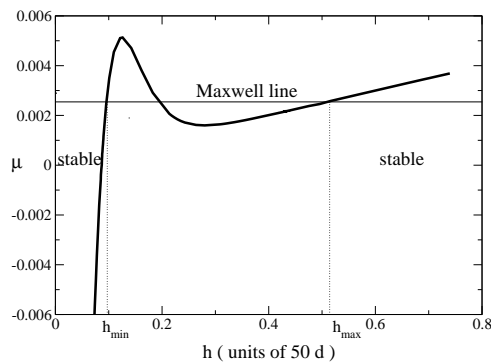
Figure 1-a,b illustrates the Maxwell construction for two different wettabilities of the solid substrate. Details regarding the numerical (kink) solutions $\rho(z)$ of Eq. (6) are given in Borcia *et al.* (2008). From the "equal area tie-line" representation one computes the liquid thicknesses h_{min} , h_{max} (binodal points) that separate the absolutely stable films (for $h < h_{min}$ and $h > h_{max}$) from the unstable/metastable films ($h_{min} < h < h_{max}$).

The liquid-solid interaction force depends on the thickness h . The stability in very thin liquid films ($h < 0.1 \mu m$) is explained by the presence of the attractive molecular component or/and the electrical component of the disjoining pressure, acting at the solid boundary. In thick liquid layers (bigger than $\cong 0.1 \mu m$), the influence of van der Waals forces is negligible. In this case, for large enough liquid depths, the gravitational force stabilizes the layer.

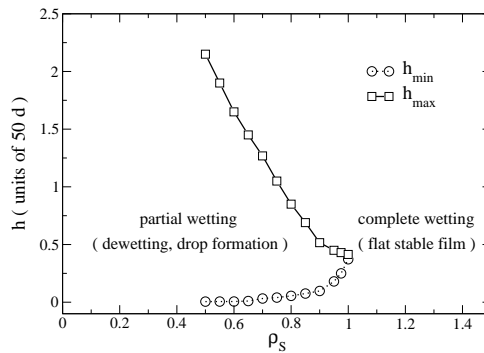
For a liquid thickness between h_{min} and h_{max} a small disturbance in the system is enough to trigger pattern formation and droplet nucleation. Increasing ρ_s , the two equal areas – above and below the Maxwell line – became smaller and, finally, reduce to a single point for hydrophilic surfaces $\rho_s \rightarrow 1$. Repeating the Maxwell construction for different wettabilities at the solid substrate, one can display the complete diagram of the liquid film stability (Figure 1-c). The binodal points h_{min} , h_{max} depicted in Figure 1-c (as functions of ρ_s) separate the partial wetting area characterized by dewetting phenomena/drop formation from the complete wetting area where the films are absolutely stable.



(a)



(b)



(c)

Figure 1: Chemical potential μ versus film thickness h for substrates with different wettabilities: (a) $\rho_s = 0.9$, (b) $\rho_s = 0.5$. The unit d represents a characteristic length of the diffuse interface. The Maxwell construction gives the binodal points that separate the partial wetting area from the complete wetting area. (c) Binodals h_{min} , h_{max} as function of ρ_s .

4 Coarsening and controlled pattern formation

Now we investigate in three dimensions the breakup of a liquid film into drops for homogeneous solid supports. Furthermore, we design liquid structures on heterogeneous solid supports adequately patterned chemically.

We solve (4) and (5) numerically using a code based on a finite-difference method (Besthorn 2006) with a mesh of $200 \times 200 \times 100$ points. A similar code was developed earlier for 2D phase field models describing floating liquid droplets with an applied temperature gradient (Borcia and Besthorn 2007). A good convergence of the numerical code is achieved for meshes with more than 100 points in one direction. In this way one assures more than 7 – 10 lattice points in the diffuse interface.

The system is bounded in the vertical direction and in the lateral direction periodic boundary conditions are taken. At the top boundary we assume $\rho = 0$, $\vec{v} = 0$. The solid boundary is placed on the bottom where $\rho = \rho_s$, $\vec{v} = 0$.

As initial condition we take a flat liquid layer of thickness h_0 with density $\rho = 1$ in a vapor atmosphere with $\rho = 0$. The whole system is at rest ($\vec{v} = 0$, everywhere). The flat liquid film is destabilized adding to the density field a small disturbance $a\xi$, with noise amplitude $a = 0.001$ and a uniformly random distribution $\xi(x, y, z)$ between 0 and 1. For $h_0 = 13d$ and a homogeneous solid boundary with $\rho_s = 0.3$ the liquid layer is unstable (Figure 1-c). The thin film breaks up in small droplets that nucleate until one drop remains. The transition from film to drop is illustrated in Figure 2 through iso-density surface snapshots.

Very recent experiments show that coarsening can be avoided or controlled by pinning effects on heterogeneous supports that are chemically patterned, see Mukherjee *et al.* (2008). A functional surface is numerically "realized" by alternating hydrophobic ($\rho_s < 0.5$) with hydrophilic ($\rho_s > 0.5$) spot in an adequate way. After the film breakup, the dewetted droplets tend to occupy the substrate regions with higher wettability. For thin liquid films ($h_0 < 20d$) stable regular structures (for example perfect squares in Figure 3-f) can be obtained as final dewetted morphology on a functional surface. Increasing the film thickness or decreasing the scale of the hydrophilic spots one loses the perfect ordering in the system because of overflow, as illustrated in Figure 4 for a thick liquid film ($h_0 = 30d$) on a functional surface with square-shaped hydrophilic patterns (as in Figure 3). How one can observe from Figure 4, as well as in the experiments performed by Mukherjee *et al.* (2008), in thicker liquid layers dewetting processes still appear, but there are uncorrelated to the substrate pattern. However, for a narrow range of the initial liquid film thicknesses, by the appropriate design of chemically patterned substrates, one can effectively "program" microfluidic devices so that the system can perform a

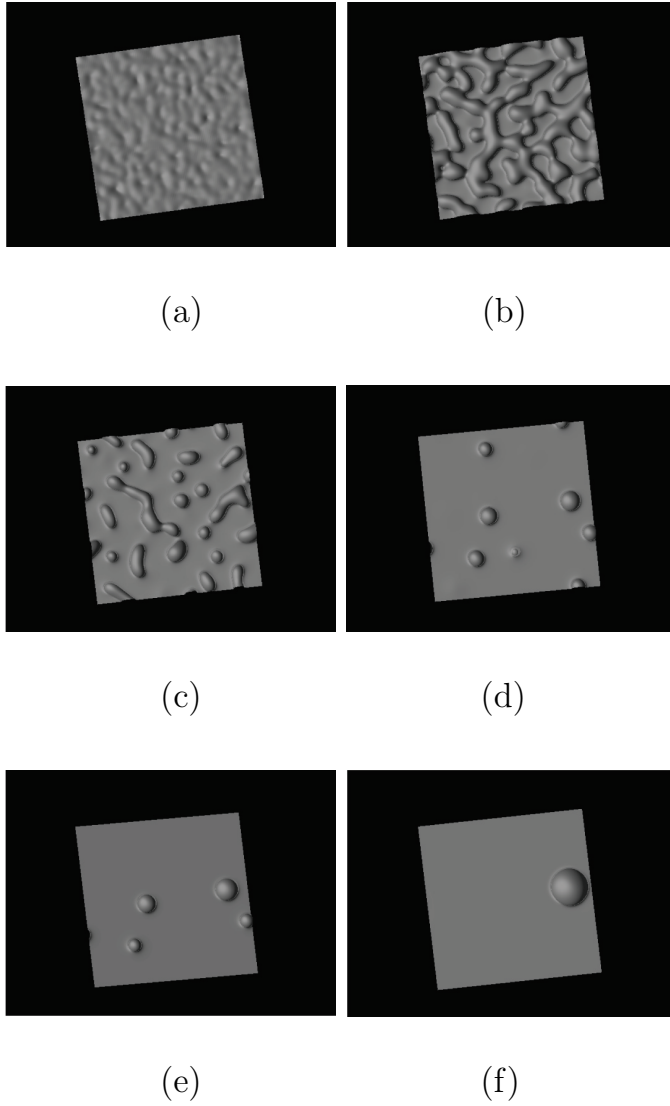


Figure 2: Transitions in a thin, unstable liquid film on a flat, homogeneous solid substrate under gravity effects ($h_0 = 13d$, $\rho_s = 0.3$): (a) $t = 50$; (b) $t = 250$; (c) $t = 500$; (d) $t = 1300$; (e) $t = 2400$; (f) $t = 6300$. The scaled time is around 10^{-11} s and the characteristic length $d = 1$ nm.

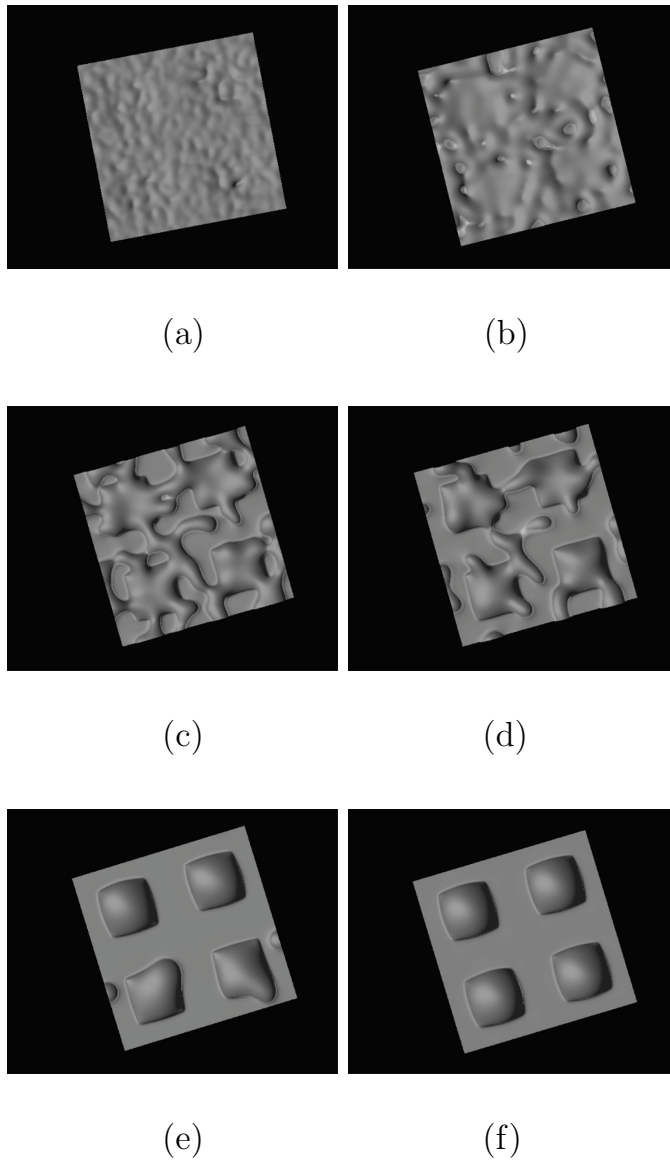


Figure 3: Transitions in a thin unstable liquid layer lying on a hydrophobic substrate ($\rho_{s1} = 0.2$) chemically patterned with hydrophilic square spots ($\rho_{s2} = 0.9$), $h_0 = 16d$: (a) $t = 50$; (b) $t = 150$; (c) $t = 450$; (d) $t = 1050$; (e) $t = 2200$; (f) $t = 5400$. The scaled time is around 10^{-11} s and the characteristic length $d = 1$ nm.

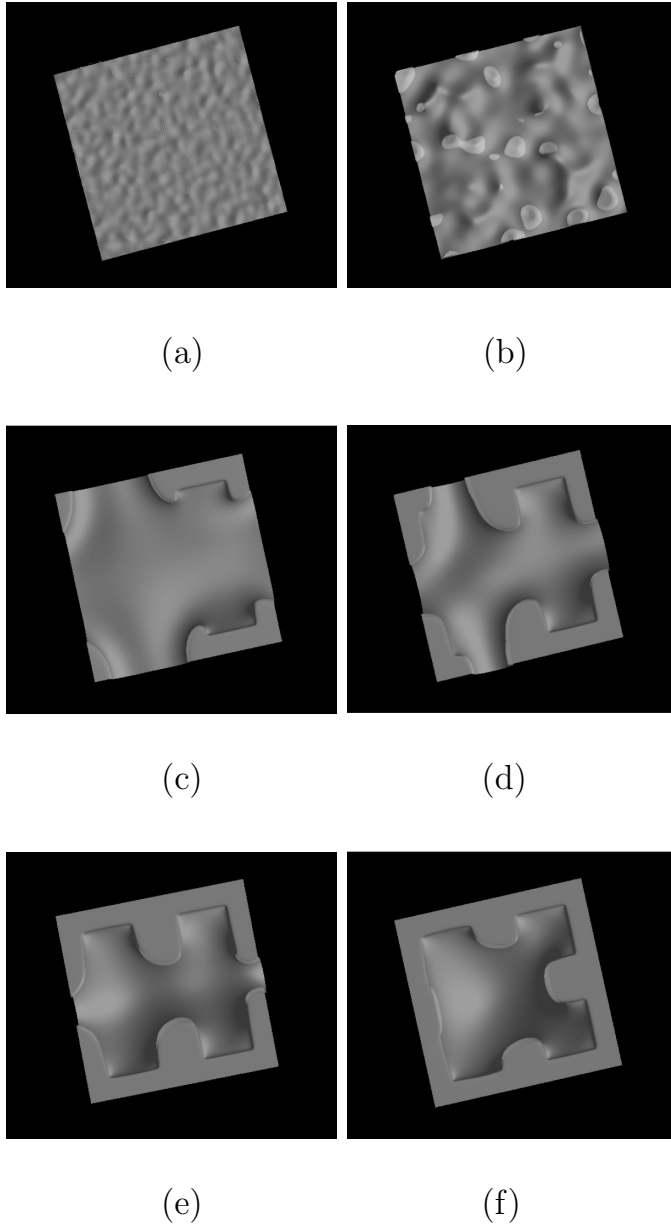


Figure 4: The same as Fig. 3 but now for a thicker liquid layer ($h_0 = 30d$): (a) $t = 50$; (b) $t = 200$; (c) $t = 2600$; (d) $t = 3900$; (e) $t = 8000$; (f) $t = 15000$. The scaled time is around 10^{-11} s and the characteristic length $d = 1$ nm.

number of functions in an autonomous manner. The patterned surface constitutes a "code". The unstable fluid flowing over the surface can be used to decode this information. Once the surface has been patterned, no external controls (other than an imposed flow) are needed to steer the system. This is an alternative to laboratory-on-a-chip methods where liquid droplets are actively manipulated by an array of electrodes in the substrate (Pollack *et al.* 2002; Schwartz *et al.* 2004).

5 Conclusions

Summarizing, we explained the formation of 3D drops near a three-phase contact line (solid-liquid-vapor) using a phase field model. We investigated the stability of a thin liquid film on a flat homogeneous solid support with variable wettability under gravity effects. We determined the critical height, below which a flat film becomes unstable on a hydrophobic/hydrophilic surface. Finally, for adequately designed solid substrates our phase field simulations are able to model controlled pattern formation of liquid structures.

Acknowledgement: This work was partially supported by the European Space Agency under AO-99-110 CIMEX project (Convection and Interfacial Mass Exchange) and partially by the Deutsche Forschungsgemeinschaft.

References

- Alexeev, A.; Balazs, A.C.** (2007): Designing smart systems to selectively entrap and burst microcapsules, *Soft Matter*, vol. 3: pp. 1500-1505.
- Bessonov, N.; Pojman, J.A.; Volpert, V.** (2004): Modelling of diffuse interfaces with temperature gradients, *J. Engn. Math.*, vol. 49: pp. 321-338.
- Bestehorn, M.; Neuffer, K.** (2001): Surface patterns of laterally extended thin liquid films in three directions, *Phys. Rev. Lett.*, vol. 87: 046101-1-4.
- Bestehorn, M; Pototsky, A; Thiele, U** (2003): 3D Large scale Marangoni convection in liquid films, *Eur. Phys. J. B*, vol. 33: pp. 457-467.
- Bestehorn, M.** (2006): *Hydrodynamik und Strukturbildung*. Springer-Verlag & Berlin Heidelberg.
- Borcia, R.; Bestehorn, M.** (2003): Phase-field model for Marangoni convection in liquid-gas systems with deformable interface, *Phys. Rev. E*, vol. 67: pp. 066307-1-10.
- Borcia, R., Bestehorn, M.** (2005): Phase-field simulations for evaporation with convection in liquid-vapor systems, *Eur. Phys. J. B*, vol. 44: pp. 101-108.

Borcia, R.; Bestehorn, M. (2007): Phase field models and Marangoni flows, *FDMP: Fluid Dynamics & Materials Processing*, vol. 3: pp. 287-293.

Borcia, R.; Borcia, I.D.; Bestehorn, M. (2008): Drops on an arbitrarily wetting substrate: A phase field description, *Phys. Rev. E*, vol. 78: pp. 066307-1-6.

Bray, A.J. (1994): Theory of phase-ordering kinetics, *Adv. Phys.*, vol. 43: pp. 357-459.

Cahn, J.W.; Hilliard, J.E. (1958): Free energy of a nonuniform system. I. Interfacial free energy, *J. Chem. Phys.*, vol. 28: pp. 258-267.

Gennes, P.G. (1985): Wetting : statics and dynamics, *Rev. Mod. Phys.*, vol. 57: pp. 827-863.

Starov, V.M.; Velarde, M.G.; Radke, C.J. (2007): *Wetting and spreading dynamics*. CRC Press Taylor & Francis Group, Boca Raton.

Jasnow, D.; Viñals, J. (1996): Coarse-grained description of thermo-capillary flow, *Phys. Fluids*, vol. 8: pp. 660-669.

Korteweg, D.J. (1901): Sur la forme que prennent les equations du mouvement des fluides si lon tient compte des forces capillaires causees par des variations de densite considerables mais connues et sur la theorie de la capillarite dans l'hypothese d'une variation continue de la densite, *Arch. Sci. Phys. Nat.*, vol. 6: pp. 1-24.

Mukherjee, R.; Bandyopadhyay, D.; Sharma, A. (2008): Control of morphology in pattern directed dewetting of thin polymer films, *Soft Matter*, vol. 4: pp. 2086-2097.

Pototsky, A; Bestehorn, M; Thiele, U (2004): Alternative pathways of dewetting for a thin liquid two-layer film, *Physica D*, vol. 199: pp. 138-148.

Pismen, L.M.; Thiele, U (2006): Asymptotic theory for a moving droplet driven by a wettability gradient, *Phys. Fluids*, vol. 18: 042104-1-10.

Pismen, L.M.; Pomeau, Y. (2000): Disjoining potential and spreading of thin layers in the diffuse-interface model coupled to hydrodynamics, *Phys. Rev. E*, vol. 62: pp. 2480-2492.

Pollack, M.G.; Shenderov, A.D.; Fair, R.B. (2002): Electrowetting-based actuation of droplets for integrated microfluidics, *Lab Chip*, vol. 2: pp. 96-101.

Pojman, J.A.; Whitmore, C.; Liveri, M.L.T.; Lombardo, R.; Marszalek, J.; Parker, R.; Zoltowski, B. (2006): Evidence for the existence of an effective interfacial tension between miscible fluids: Isobutyric acid-water and 1-butanol-water in a spinning-drop tensiometer, *Langmuir*, vol. 22: pp. 2569-2577.

Scheid, B.; Oron, A.; Colinet, P.; Thiele, U.; Legros, J.C. (2002): Nonlinear evolution of nonuniformly heated falling liquid films, *Phys. Fluids*, vol. 14: pp. 4130-4151.

Schwartz, J.A.; Vykoukal, J.V.; Gascoyne, P.R.C. (2004): Droplet-based chemistry on a programmable micro-chip, *Lab Chip*, vol. 4: pp. 11-17.